Neuron, Volume *86*

Supplemental Information

Genetic Differences in the Immediate Transcriptome Response to Stress Predict Risk-Related Brain Function and Psychiatric Disorders

Janine Arloth, Ryan Bogdan, Peter Weber, Goar Frishman, Andreas Menke, Klaus V. Wagner, Georgia Balsevich, Mathias V. Schmidt, Nazanin Karbalai, Darina Czamara, Andre Altmann, Dietrich Trümbach, Wolfgang Wurst, Divya Mehta, Manfred Uhr, Torsten Klengel, Angelika Erhardt, Caitlin E. Carey, Emily Drabant Conley, Major Depressive Disorder Working Group of the Psychiatric Genomics Consortium (PGC), Andreas Ruepp, Bertram Müller-Myhsok, Ahmad R. Hariri, and Elisabeth B. Binder

SUPPLEMENTAL DATA

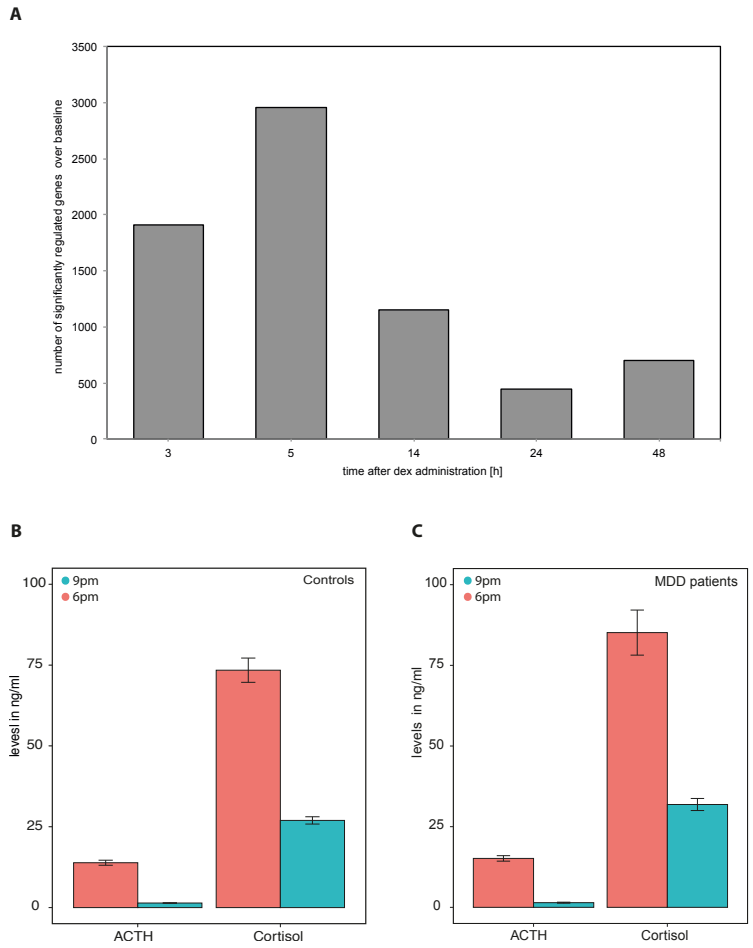

Figure S1. Related to Figure 2.

(A) Time course of gene expression changes after oral dexamethasone administration. The number of genes that are differently expressed at several time points after administration of 1.5 mg dexamethasone relative to baseline in 4 healthy male individuals are shown. The height of the bars indicates the total number of transcripts with nominally significant changes from baseline gene expression. Baseline blood samples were obtained at 6pm. This evening time point was chosen so that the stimulation experiments took place during the quiescent period of the stress hormone system. Baseline blood draws were immediately followed by oral administration of dexamethasone. Additional blood samples were drawn at 9pm and 11pm on the same day, at 8am and 6pm the next day and at 6pm on day 3. A comparison of baseline gene expression vs. gene expression after 3, 5, 14, 24 and 48 h shows an initial high number of gene expression changes, followed by a normalization within 24-48 hours. The highest number of differently expressed genes (highest bar in chart) was observed at 3 and 5 hours post dexamethasone ingestion. For practical reasons as well as to avoid secondary GR target effects, in the subsequent experiment we collected blood 3 hours after dexamethasone intake. (B), (C) Dexamethasone effect on cortisol and ACTH levels. Administration of dexamethasone resulted in a robust suppression of cortisol in all individuals. Cortisol levels were significantly suppressed in healthy controls (B; $F_{1,90} = 89.74$, $P = 3.57 \times 10^{-15}$) as well as in depressed patients (C; $F_{1,67} = 7.09$, $P = 0.0097$) 3h after dexamethasone challenge. Similar results were observed for ACTH, with a significant reduction in ACTH levels in healthy controls B; $F_{1,91} = 43.96$, $P = 2.33 \times 10^{-9}$) and in depressed patients (C; $F_{1,65} = 9.75$, $P = 0.0027$) after 3h.

P values in (A,B) derived from a linear model; error bars: ± sem

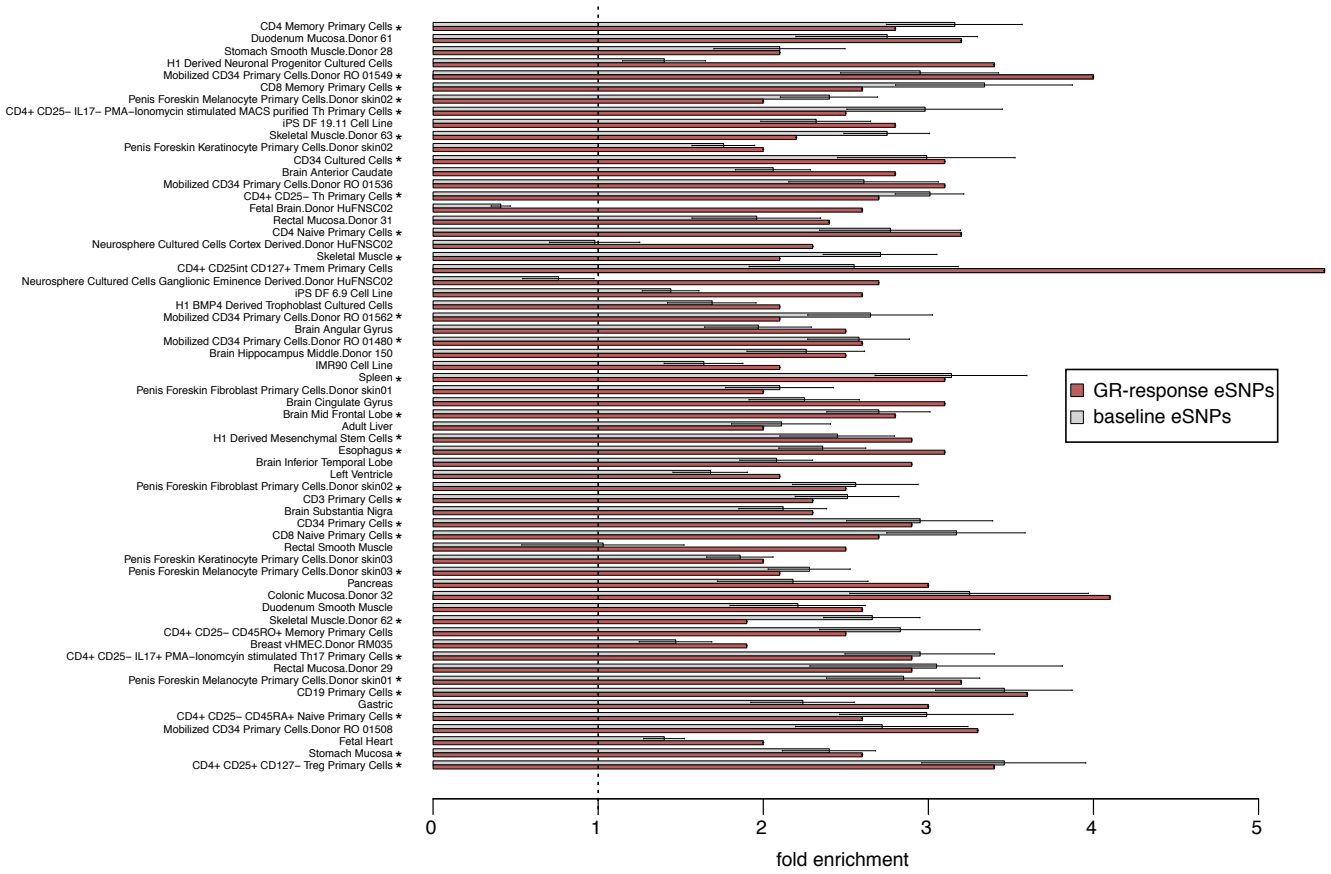

Figure S2. Related to Figure 3.

GR- eSNPs are enriched for enhancers in multiple tissues and cell lines from the Roadmap Epigenome Project. The x-axis shows the fold enrichment and the y-axis shows all enhancers that survived the Bonferroni multiple testing correction for the number of tested tissues or cells. GR-response eSNPs are illustrated in red and baseline eSNPs in gray. Out of the 62 presented enhancers, 28 additionally showed a significant enrichment within baseline eSNPs (marked with *).
P values derived from a binomial enrichment test; error bars: ± sd

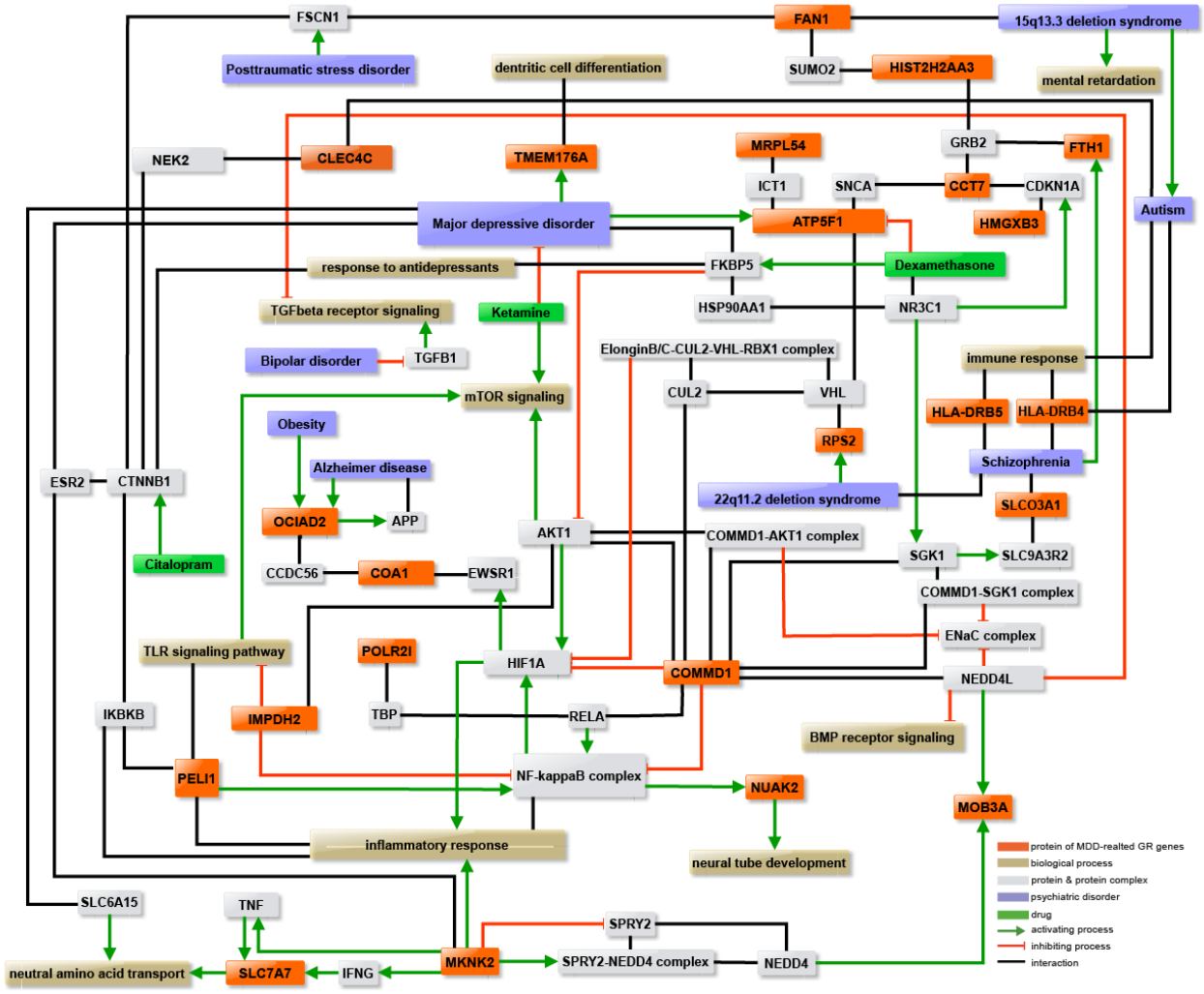

Figure S3. Related to Figure 6.
Disease-related network. For 22 of the 24 MDD-related GR genes a tightly interconnected disease-related network was generated from manually curated experimental data derived from the literature. Elements of the figure: Proteins from MDD-related GR genes (orange boxes), additional proteins and protein complexes (white boxes), biological processes (beige boxes), psychiatric disorders (blue boxes), drugs (green boxes), activating processes (green arrow-headed lines), inhibitory processes (red bar-headed lines) and interactions such as physical interactions, associations with diseases and differential regulation of signaling pathways (black line).

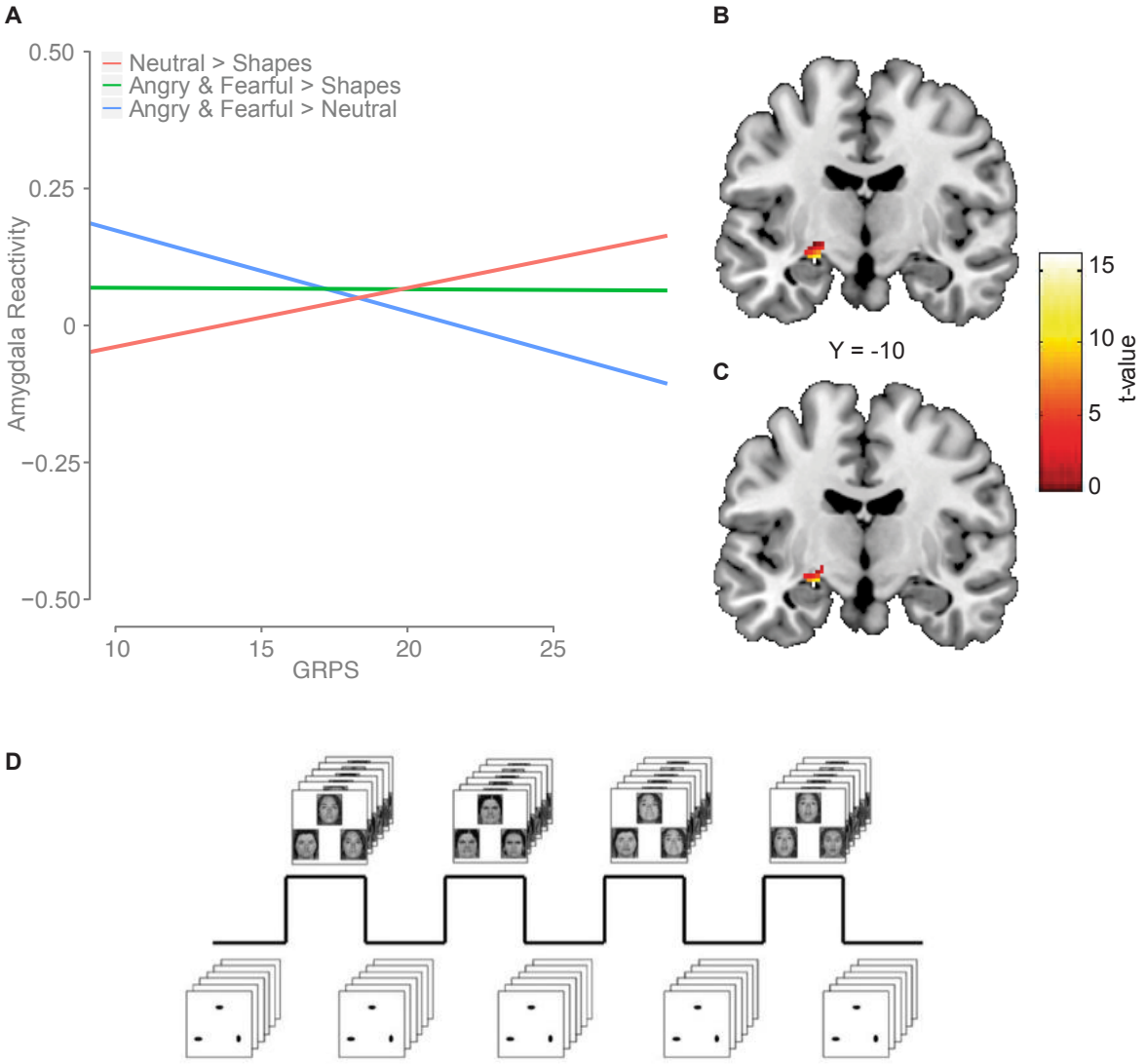

Figure S4. Related to Figure 7.
(A) Elevated genetic risk profile scores (GRPSs) correlate with dysfunctional amygdala reactivity in the entire DNS sample (*n* = 647). As previously found in the European-American subsample, elevated GRPSs predicted blunted amygdala reactivity to threat-related expressions in comparison to neutral expressions in the entire sample when controlling for patterns of population stratification. Post-hoc analyses revealed that GRPS was not predictive of reactivity to threat-related expressions, but that higher GRPSs predicted elevated amygdala reactivity to neutral expressions, in comparison to non-face control stimuli. (B), (C) Show the main effects of the post hoc contrasts for left centromedial amygdala reactivity used in imaging genetics analyses of GRPS in the entire sample. (B) "Angry & Fearful > Shapes" (49 contiguous voxels; max voxel MNI coordinate, x = -24, y = -10, z = -14, t = 22.59, $P < 4.41 \times 10^{-16}$), and (C) "Neutral > Shapes" (35 contiguous voxels; max voxel MNI coordinate, x = -24, y = -10, z = -14, t = 10.73, $P < 4.41 \times 10^{-16}$). (D) DNS fMRI Task: Participants completed four expression-specific (Neutral, Angry, Fear, Surprise) face-matching task blocks interleaved with five sensorimotor shape-matching control blocks. Order for task blocks was counterbalanced across participants.

Table S1. Related to Figure 2.
List of the 320 *cis*-eSNP-probe combinations (*cis*-eQTL bins).

(In separate Excel file.)

Table S2. Related to Figure 5. Overlap of GR-response *cis*-eSNP bin-probe combinations with SNPs nominally associated with MDD in the meta-analysis for MDD (meta-analysis $P \leq 0.05$; $n = 17,846$ samples).
List of 26 eSNP bins (23 tagging SNPs), representing the overlap of the 282 GR-response *cis*-eSNPs and SNPs from the meta-analysis for MDD.

	tag SNP eQTL b	Genes nearby tag SNP	SNP Locati	SNP Chr[a]	PGC A1[b]	PGC A2[c]	PGC OR[d]	PGC RiskA	PGC p-value[f]	P ID[g]	P Gene[h]	Q value[i]	Cross Disorder Association[j]	GR binding site
1	1-148440425	*PLEKHO1, ANP32E*	intergenic	1	T	G	1.09	T	0.013	ILMN_1695435	*HIST2H2AA3/4*	0.006	CDA, BPD, SCZ, ADHD	yes
2	19-40883657	*UPK1A, ZBTB32*	intergenic	19	C	G	0.91	G	0.001	ILMN_1720542	*POLR2I*	0.044	BPD	yes
3	rs10002500	*CNGA1*	intronic	4	T	C	1.07	T	0.043	ILMN_1700306	*OCIAD2*	0.024		no
4	rs10505733	*CLEC4C*	intronic	12	A	C	0.94	C	0.021	ILMN_1665457	*CLEC4C*	0.00021	SCZ	no
	rs10505733	*CLEC4C*	intronic	12	A	C	0.94	C	0.021	ILMN_1682259	*CLEC4C*	0.00021	SCZ	no
5	rs12432242	*SLC7A7*	intronic	14	T	C	0.94	C	0.008	ILMN_1810275	*SLC7A7*	0.041	CDA, BPD	no
6	rs12611262	*SEMA6B, TNFAIP8L1*	intergenic	19	T	C	1.06	T	0.022	ILMN_1658486	*MRPL54*	0.046		no
7	rs12620091	*ALMS1P*	ncRNA_intr	2	T	C	0.95	C	0.022	ILMN_1662954	*CCT7*	0.047		no
8	rs17239727	*BLVRA*	intronic	7	A	G	0.94	G	0.022	ILMN_2081335	*COA1*	0.024	CDA	yes
9	rs1873625	*BSN*	intronic	3	A	C	0.94	C	0.018	ILMN_1705737	*IMPDH2*	0.048		no
10	rs1981294	*LRIF1, DRAM2*	intergenic	1	T	C	1.07	T	0.021	ILMN_1721989	*ATP5F1*	0.037	CDA	no
11	rs2072443	*TMEM176B*	exonic	7	T	C	1.05	T	0.034	ILMN_1791511	*TMEM176A*	0.036		no
12	rs2269799	*SV2B*	intronic	15	T	C	0.95	C	0.04	ILMN_1663699	*SLCO3A1*	0.047		no
13	rs2395891	*BTBD2, MKNK2*	intergenic	19	T	G	1.07	T	0.031	ILMN_1721344	*MOB3A*	0.024	CDA, BPD	yes
	rs2395891	*BTBD2, MKNK2*	intergenic	19	T	G	1.07	T	0.031	ILMN_2347068	*MKNK2*	0.028	CDA, BPD	yes
14	rs2422008	*WDPCP*	intronic	2	A	C	1.05	A	0.036	ILMN_1679268	*PELI1*	0.042	CDA, ASD	yes
15	rs2956993	*GANAB*	intronic	11	T	G	0.95	G	0.032	ILMN_1746525	*FTH1*	0.044		no
16	rs35288741	*NFASC*	intronic	1	A	G	1.05	A	0.042	ILMN_2094952	*NUAK2*	0.044		no
17	rs6493387	*TRPM1*	intronic	15	T	C	0.93	C	0.001	ILMN_1778734	*FAN1*	0.045	CDA	no
18	rs6545924	*COMMD1, B3GNT2*	intergenic	2	T	G	1.06	T	0.018	ILMN_1761242	*COMMD1*	0.045		no
19	rs7194275	*C16orf91, CCDC154*	intergenic	16	T	C	0.92	C	0.021	ILMN_1688749	*RPS2*	0.049	CDA, BPD, SCZ	no
20	rs7252014	*KCNN1*	intronic	19	A	G	1.06	A	0.016	ILMN_1766487	*LRRC25*	0.038		no
21	rs917585	*SLC6A7*	intronic	5	C	G	1.05	C	0.029	ILMN_1694686	*HMGXB3*	0.045	CDA, SCZ	no
22	rs9268671	*HLA-DRA, HLA-DRB5*	intergenic	6	A	G	0.95	G	0.031	ILMN_1697499	*HLA-DRB5*	0.00021	CDA, SCZ, ASD	no
23	rs9268926	*HLA-DRA, HLA-DRB5*	intergenic	6	A	G	0.92	G	0.041	ILMN_1697499	*HLA-DRB5*	0.012	CDA, SCZ, ASD	no
	rs9268926	*HLA-DRA, HLA-DRB5*	intergenic	6	A	G	0.92	G	0.041	ILMN_2159694	*HLA-DRB4*	0.00073	CDA, SCZ, ASD, ADHD	no

[a] *SNP Chromosome*
[b] *code for allele 1 (reference allele, not necessary minor allele)*
[c] *code for allele 2*
[d] *odds ratio*
[f] *risk allele*
[f] *meta analysis p-value*
[g] *Illumina probe identifier (Human HT-12 v3)*
[h] *probe gene*
[i] *lowest Q value for eSNP bin*
[j] *probes that also had an eSNP associated with bipolar disorder (BPD), schizophrenia (SCZ), attention deficit-hyperactivity disorder (ADHD), autism spectrum disorder (ASD) or the cross disorder analysis (CDA)*
[k] *eSNP bins including a GR binding site based on ChIP-seq data*

Table S3. Related to Figure 5. MDD-related GR tagging eSNPs and their proxy SNPs used to generate the cumulative risk allele profile in the MARS cohort. Three SNPs deviated from HWE (rs12620091, rs9268671 and rs9268926) and were excluded from the analysis. As result the remaining 20 SNPs were used to generate a profile.

	tag SNP eQTL bin	Proxy for SNP[a]	Genes nearby tag SNP	SNP Chr	MARS A1[b]	MARS A2[c]	MARS MAF[c]	MARS HWE P value[e]	Used for analysis
1	1-148440425	rs72694971 (renamed)	*PLEKHO1, ANP32E*	1	G	T	0.12	0.56	yes
2	19-40883657	rs73048504 (renamed)	*UPK1A, ZBTB32*	19	C	G	0.18	0.22	yes
3	rs10002500		*CNGA1*	4	T	C	0.13	0.58	yes
4	rs10505733		*CLEC4C*	12	C	A	0.29	0.42	yes
5	rs12432242		*SLC7A7*	14	C	T	0.39	0.87	yes
6	rs12611262		*SEMA6B, TNFAIP8L1*	19	T	C	0.39	0.59	yes
7	rs12620091	rs34874205 (r^2=0.92)	*ALMS1P*	2	C	T	0.37	< 0.00001	no
8	rs17239727		*BLVRA*	7	T	C	0.21	0.48	yes
9	rs1873625		*BSN*	3	A	C	0.29	0.85	yes
10	rs1981294		*LRIF1, DRAM2*	1	C	T	0.17	0.47	yes
11	rs2072443		*TMEM176B*	7	T	C	0.41	0.75	yes
12	rs2269799		*SV2B*	15	C	T	0.32	0.23	yes
13	rs2395891		*BTBD2, MKNK2*	19	T	G	0.35	0.21	yes
14	rs2422008		*WDPCP*	2	A	C	0.43	1	yes
15	rs2956993		*GANAB*	11	G	T	0.38	0.30	yes
16	rs35288741		*NFASC*	1	G	A	0.35	0.25	yes
17	rs6493387		*TRPM1*	15	T	C	0.47	0.11	yes
18	rs6545924		*COMMD1, B3GNT2*	2	G	T	0.50	0.30	yes
19	rs7194275		*C16orf91, CCDC154*	16	C	T	0.12	0.0007	yes
20	rs7252014		*KCNN1*	19	A	G	0.48	0.054	yes
21	rs917585		*SLC6A7*	5	G	C	0.50	0.57	yes
22	rs9268671	rs116072659 (renamed)	*HLA-DRA, HLA-DRB5*	6	A	G	0.34	< 0.00001	no
23	rs9268926	rs114766558 (r^2=0.81)	*HLA-DRA, HLA-DRB5*	6	G	A	0.31	< 0.00001	no

[a] *r^2=LD from MPIP cohort*

[b] *code for allele 1 (reference allele, not necessary minor allele)*

[c] *code for allele 2*

[d] *minor allele frequency*

[e] *Hardy-Weinberg test statistics*

Table S4. Related to Figure 7 and S3. MDD-related GR tagging eSNPs and their proxy SNPs used to generate the cumulative risk allele profile in the DNS cohort. Four SNPs did not have a proxy available (rs12620091, rs917585, rs9268671 and rs9268926). No SNPs deviated from HWE.

							DNS MAF[d]		DNS HWE P values[e]					
	tag SNP eQTL bin	Proxy for SNP[a]	Genes nearby tag SNP	SNP Chr	DNS A1[b]	DNS A2[c]	EUR-AM	ALL	EUR-AM	AFR-AM	Latino/a	Asian1	Asian 2	Used in the analysis
1	1-148440425	rs11588837 (r^2=0.96)	*PLEKHO1, ANP32E*	1	A	G	0.15	0.34	0.48	0.95	0.34	0.99	0.72	yes
2	19-40883657	rs8106959 (r^2=0.95)	KMT2B	19	A	G	0.22	0.18	0.53	0.89	0.87	0.28	0.5	yes
3	rs10002500		*CNGA1*	4	T	C	0.1	0.19	0.28	0.74	0.65	0.48	0.5	yes
4	rs10505733	rs1894823 (r^2=1)	*CLEC4C*	12	T	C	0.31	0.28	0.34	0.4	0.16	0.14	0.35	yes
5	rs12432242	rs2281677 (r^2=0.93)	*SLC7A7*	14	A	G	0.38	0.39	0.96	0.29	0.04	0.16	0.31	yes
6	rs12611262		*SEMA6B, TNFAIP8L1*	19	T	C	0.37	0.44	0.49	0.84	0.57	0.26	0.55	yes
7	rs12620091	no Proxy												no
8	rs17239727	rs10229363 (r^2=1)	*BLVRA*	7	A	G	0.2	0.13	0.23	0.62	0.47	0.86	0.35	yes
9	rs1873625	rs9858280 (r^2=1)	*BSN*	3	T	C	0.37	0.28	0.39	0.6	0.71	0.52	0.24	yes
10	rs1981294	rs4838884 (r^2=1)	*LRIF1, DRAM2*	1	A	G	0.2	0.19	0.63	0.66	0.48	0.932	0.67	yes
11	rs2072443		*TMEM176B*	7	T	C	0.42	0.44	0.38	0.41	0.59	0.39	0.74	yes
12	rs2269799		*SV2B*	15	C	T	0.33	0.35	0.1	0.6	0.32	0.5	0.35	yes
13	rs2395891		*BTBD2, MKNK2*	19	T	G	0.34	0.38	0.49	0.18	0.26	0.3	0.03	yes
14	rs2422008		*WDPCP*	2	A	C	0.47	0.41	0.85	0.25	0.9	0.13	0.82	yes
15	rs2956993		*GANAB*	11	G	T	0.35	0.29	0.42	0.47	0.43	0.61	0.99	yes
16	rs35288741	rs7534993 (r^2=1)	*NFASC*	1	G	A	0.34	0.27	0.24	0.21	0.56	0.53	0.35	yes
17	rs6493387	rs12901022 (r^2=1)	*TRPM1*	15	C	T	0.48	0.46	0.79	0.44	0.41	0.94	0.82	yes
18	rs6545924	rs921320 (r^2=1)	*COMMD1, B3GNT2*	2	C	A	0.5	0.5	0.17	0.53	0.4	0.65	0.94	yes
19	rs7194275		*C16orf91, CCDC154*	16	C	T	0.19	0.19	0.5	0.92	0.73	0.051	1	yes
20	rs7252014		*KCNN1*	19	A	G	0.48	0.47	0.55	0.37	0.31	0.07	0.45	yes
21	rs917585	no Proxy												no
22	rs9268671	no Proxy												no
23	rs9268926	no Proxy												no

[a] *r^2=LD for CEU population from 1KGP (>0.90 for all subpopulations)*

[b] *code for allele 1 (i.e., reference risk allele, not necessary minor allele)*

[c] *code for allele 2*

[d] *minor allele frequencies*

[e] *Hardy-Weinberg test statistics for European Americans (EUR-AM), African Americans (AFR-AM), Latino/as, Asian Cluster 1 (Asian1) and Asian Cluster 2 (Asian2)*

Table S5. Related to Figure 7 and S3. Psychiatric Diagnoses in the Duke Neurogenetics Study (DNS). Of note, this table represents the number of diagnoses across DNS participants. Some individuals presented with a comorbid status.

	European American (*n*=306)	Full Sample (*n*=647)
Alcohol Abuse	22	41
Alcohol Dependence	19	31
Major Depressive Disorder	8	17
Marijuana Abuse	7	15
Gernalized Anxiety Disorder	7	11
Social Anxiety Disorder	3	8
Agoraphobia w/o Panic Disorder	6	8
Bipolar Disorder NOS	6	8
Marijuana Dependence	5	7
Bipolar II	3	6
OCD	4	6
Bulimia Nervosa	2	5
Panic Disorder	1	4
Dysthymia	0	1
PTSD	0	1
Anorexia Nervosa	0	1
Bipolar I	1	1
TOTAL	94	171

Table S6. Related to Figure 2. Sequence of primers used in this study.

List of primers and universal probe library number used for the qPCR for *ADORA3*, *HIST2H2AA3/4* and *TBP* in human whole blood.

Target Gene	Primer Set (5'-3')	UPL probe number
ADORA3	Forward: tcatttgcagccaggtagc	82
	Reverse: tgcttgggtgtggtctatca	
HIST2H2AA3, HIST2H2AA4 (short isoform)	Forward: cgacgaggaactgaacaagc	61
	Reverse: gcctggatgttaggcaagac	
HIST2H2AA3, HIST2H2AA4 (long isoform)	Forward: aaggggcacctgtgaactc	21
	Reverse: gactgagagtggccagcatt	
TBP	Forward: ctttgcagtgacccagcat	67
	Reverse: cgctggaactcgtctcacta	

List of primers used for the qPCR for *LONP1* and *GAPDH* in LCLs.

Target Gene	Primer Set (5'-3')
LONP1	Forward: TTGGTGGCATCAAGGAGAAG
	Reverse: CGGTAGTGTTCCACGAAGTG
GAPDH	Forward: CCAAGGTCATCCATGACAAC
	Reverse: GAGGCAGGGATGATGTTCTG

Oligonucleotides for Chromatin Conformation Capture (3C).

Primer	Sequence
C1	GCCTTACCCAGCACATTTTG
P1	CTGGAAGAGCTTGACCAAGTG
P2	CTCACTCCCCTTGCAATCTC
P3	ACTCGCTTTTTGCAGTAGGG
P4	TACCGCAGCCTACTGCATC
P5	CTTCCACACTGAATCTCACCTG
P6	ATCAATGACCCTCACTCCTCTC
P6	ATCAATGACCCTCACTCCTCTC

Primer set for DNA quantification of 3C samples.

Primer Set (5'-3')
Forward: TGGTGAAACCCCGTCTCTAC
Reverse: AATCTCAGCTCACTGCAACC

SUPPLEMENTAL EXPERIMENTAL PROCEDURES

Samples and study design.

MPIP cohort.

The subject pool for the eQTL analysis consisted of 164 male Caucasian individuals (90% of German origin) recruited for the MARS project (Ising et al., 2009): 93 healthy probands (age = 40.2 ± 12.4 years; body mass index (BMI) = 24.9 ± 3.1 kg/m^2) and 71 in-patients with MDD (age = 48.5 ± 13.5 years; HAM-D = 25.3 ± 8.0; BMI = 26.1 ± 3.6 kg/m^2). All were treated at the hospital of the Max Planck Institute of Psychiatry in Munich, Germany (MPIP; MPIP cohort). Only individuals not reporting a history of current psychiatric, major neurological nor general medical disorders were included in the control sample. Recruitment strategies and further characterization of the MPIP cohort have been described previously (Hennings et al., 2009; Menke et al., 2012). Of these participants, 4 were excluded due genotyping problems.

MARS cohort. This sample included 1,005 MDD patients (561 female, 444 males; age = 48.15 ± 14.13 years; HAM-D = 25.68 ± 6.5), as well as 478 controls (298 females, 180 males; age = 47.83 ± 13.7 years), recruited for the MARS project at the MPIP in Munich, Germany. All included patients were of European descent. Recruitment strategies and further characterization including population stratification of the MARS cohort have been described previously (Hennings et al., 2009; Menke et al., 2012). All individuals used within the eQTL study (MPIP cohort) were not part of this sample.

DNS cohort.

All participants from the Duke Neurogenetics Study (DNS) provided informed written consent, prior to participation, in accord with the guidelines of the Duke University Medical Center Institutional Review Board. All participants were in good general health and free of the following DNS exclusion criteria: (1) medical diagnosis of cancer, stroke, diabetes requiring insulin treatment, chronic kidney or liver disease or lifetime psychotic symptoms; (2) use of psychotropic, glucocorticoid or hypolipidemic medication, and (3) conditions affecting cerebral blood flow and metabolism (e.g., hypertension). Current DSM-IV Axis I and select Axis II disorders (Antisocial Personality Disorder

and Borderline Personality Disorder) were assessed with the electronic Mini International Neuropsychiatric Interview (Sheehan et al., 1998) and Structured Clinical Interview for the DSM-IV Axis II (SCID-II) (First et al., 1997) respectively. These disorders are not exclusionary as the DNS seeks to establish broad variability in multiple behavioral phenotypes related to psychopathology.

On January 6th, 2014, 726 participants had overlapping fMRI and genetic data that was fully processed and used for these analyses. Of these participants, 79 were excluded due to scanner-related artifacts in fMRI data (*n* = 6), incidental structural brain abnormalities (*n* = 2), a large number of movement outliers in fMRI data (*n* = 21; see ART description below), inadequate signal in our amygdala regions of interest (*n* = 14; see coverage description below), poor behavioral performance (*n* = 20; accuracy lower than 75%), outlier status according to ancestrally-informative principal components (*n* = 5), scanner malfunctions (*n* = 2), incomplete fMRI data collection (*n* = 1), and failed genotyping at one GRPS polymorphisms (without a proxy of $r^2 > 0.9$; *n* = 8). Thus, all imaging genetics analyses were conducted in a final European-American subsample of 306 participants (age = 19.72 ± 1.23 years; 148 males; 63 with DSM-IV Axis I disorder) and a full sample of 647 participants (age = 19.65 ± 1.24 years; 285 males; 117 with DSM-IV Axis I disorder; 306 European Americans, 72 African Americans, 170 Asians, 37 Latino/as, and 62 of Other/Multiple racial origins according to self-reported ethnicity; for a full description of diagnoses present in the sample see Table S5).

Mouse models.

The animal experiments were carried out in the animal facilities of the MPIP in Munich, Germany. Male C57BL/6N mice at an age of 12 weeks (mean bodyweight 26.8 ± 0.1 g) were used for the dexamethasone-stimulation test (DEX-mouse). The experiment was performed twice with two separate batches of mice (*n* = 22 per batch). Male 3-4 month old C57BL/6N mice (mean bodyweight 25.5 ± 2.12 g) were used for the acute social defeat mouse model (Stress-mouse). Two weeks before the experiment onset, mice were singly housed and

acclimated to the experimental room. All mice (DEX and Stress-mice) were kept under a 12 h light/dark cycle and standard conditions. Food and tap water were available *ad libitum*. All efforts were made to minimize animal suffering during the experiment. The committee for the Care and Use of Laboratory animals of the Government of Upper Bavaria, Germany approved the protocols.

(i) DEX-mouse: Animals were injected i.p. with either vehicle (VEH, *n* = 11) or 10 mg/kg dexamethasone (DEX, *n* = 11) between 9am and 11am. Animals were sacrificed 4 hours post injection, blood was collected and the brains were carefully removed. The prefrontal cortex (PFC; batch 1), hippocampus (HC; batch 1) and amygdala (AM; batch 2) were dissected immediately according to standard protocols (Spijker, 2011). Amygdala preparation was as follows: brains were cut into ca. 1 mm thick slices using a custom-mounting device. The amygdala (all subnuclei) (Paxinos and Franklin, 2003) was manually dissected with a scalpel under visual control using a binocular microscope. HC and PFC preparation: brain regions were manually dissected from the whole brain by trained personnel. Dissected tissues were directly transferred into RNA lysis solution (Applied Biosystems, USA) and frozen at -80°C. In addition, 300 µl of trunk blood (batch 1) was collected into microcentrifuge tubes containing PaxGene RNA stabilizer solution and frozen at -20°C.

(ii) Stress-mouse: The acute social defeat stress paradigm lasted 5 min and was conducted as previously described (Wagner et al., 2013). Briefly, experimental mice were placed in the home cage of a dominant aggressive CD1 resident mouse. Interaction between the mice was permitted for 5 min without any interference unless an animal was severely injured. When this was the case, the experimental animal was returned to his home cage and excluded from analysis. Prior to the experimental day, all CD1 resident mice received aggression tests to ensure dominance and were trained for aggressive behavior. The control mice were allowed to explore an empty cage (control condition) for 5 min. Exactly 4 h after

the onset of the stress paradigm, the mice were sacrificed and the tissue harvested for subsequent analyses. Briefly, mice were anesthetized with Isofluorane and then immediately killed by decapitation. In the same manner as for the DEX-mouse, 250µl of trunk blood was collected and the brains were carefully removed. The same brain regions i.e. the HC, AM and PFC were dissected out, snap-frozen, and stored in RNA lysis solution at -80°C until needed.

Gene expression data.

Human whole blood of the MPIP cohort was collected using PAXgene Blood RNA Tubes (PreAnalytiX), processed as described previously (Menke et al., 2012) and hybridized to Illumina HumanHT-12 v3.0 Expression Bead Chips. Samples had a mean RNA integrity number (RIN) of 7.97 ± 0.42 *SD*. The Illumina Bead Array Reader was used to scan the microarrays and summarized raw probe intensities were exported using Illumina's GenomeStudio v2011.1 Gene Expression module. Further processing was carried out using R version 2.14.0 (http://www.r-project.org/). All 48,750 probes present on the microarray were first filtered by an Illumina detection *P* value of 0.01 in at least 10% of the samples, leaving 14,168 expressed probes for further analysis. Each transcript was then transformed and normalized through variance stabilization and normalization (VSN) (Lin et al., 2008). Technical batches were adjusted using ComBat with fixed effects of amplification round (Johnson and Cheng, 2007). To test for hidden confounding effects within the ComBat corrected data, we applied a surrogate variable analysis (Leek and Storey, 2007). No significant surrogate variable could be identified suggesting that most of the confounding effects were captured by correcting for known batch effects. To further reduce batch effects baseline and dexamethasone stimulated RNA samples for each individual were processed within a single run. Finally for each probe, we constructed a linear model of the log fold change in gene expression between 6pm (baseline) and 9pm (GR-stimulation) standardized

to 6pm (baseline) controlling for age, disease status and BMI. Models were implemented in "R" using the "lm" function. The residuals (GR-response residuals) from this regression were used as phenotype values in the following analyses. The results did not change when the RIN factor, the dexamethasone serum levels (3 hours following administration) and the differential blood cell count (levels of monocytes, granulocytes and lymphocytes) were included as additional independent covariates.

To control if significant eQTLs might be biased due to SNPs within the probes, the Illumina re-annotation pipeline (ReMOAT version August 2009) (Barbosa-Morais et al., 2010) was used to annotate SNPs (relying on UCSC dbSNP 126 table) that were located within the gene expression probe sequence. No bias of eQTL misclassifications due to such sequence polymorphisms in the probe region could be identified. The probe gene names were updated using the NCBI build 36 (hg18) Reference Sequence (RefSeq) (Pruitt et al., 2012) gene annotation table obtained from the UCSC Table Browser (http://hgdownload.soe.ucsc.edu/goldenPath/hg18/database/refGene.txt.gz). The positions of the probes were annotated using ReMOAT and only autosomal probes were used for the GR-response eQTL analysis (n = 4,447 autosomal probes).

DEX-mouse und Stress-mouse RNA was extracted from whole blood using the PAXgene blood miRNA kit (PreAnalytiX) according to (Krawiec et al., 2009). RNA was extracted from the mouse brain regions using RNeasy Plus Universal Mini Kit (Qiagen) in the DEX-mouse experiment and using TRIzol (Life Technologies) in the Stress-mouse experiment, both according to manufacturer's protocol. RNA was quality checked using the Agilent 2100 Bioanalyser, amplified using the Illumina Total Prep 96-Amplification kit (Life Technology) and then hybridized on Illumina MouseRef-8 v2.0 (for DEX-mouse) and Illumina MouseWG-6 v2.0 BeadChips (for Stress-mouse). For each tissue and experiment the samples were processed together (RNA amplification, hybridization and scanning). All samples had a mean RIN of 7.5 ± 0.2 *SD* for DEX-mouse and 6.6 ± 0.5 *SD* for Stress-mouse

blood cells and a mean RIN of 9.2 ± 0.4 *SD* for DEX-mouse and 9.2 ± 0.3 *SD* Stress-mouse brain tissues. All probes present on the microarrays (MouseRef-8 = 25,700; MouseWG-6 = 45,200 probes) were first filtered using an Illumina detection *P* value of 0.05 in at least 15% of the samples. Secondly, each transcript was transformed, normalized and batch corrected, in the same fashion as for the human gene expression data. For differential gene expression analysis between the VEH and DEX animals, as well as between control and stress animals linear regression models implemented in R were used on the normalized, transformed and batch corrected expression values for each tissue. Multiple testing corrections were performed by controlling the false discovery rate (*FDR*) according to Benjamini and Hochberg. A *FDR* ≤ 10% was considered as significant. Results were illustrated as a heatmap in Figure 6B. If multiple array probes per gene existed, only the most significant one is shown in Figure 6B.

Genotype data.

Human DNA of the MPIP cohort samples was isolated from EDTA blood samples using the Gentra Puregene Blood Kit (Qiagen) with standardized protocols. Genome-wide SNP genotyping was performed using Illumina Human610-Quad and Illumina Human660W-Quad Genotyping BeadChips according to the manufacturer's standard protocols. In total, 582,539 genetic markers in 163 individuals of the MPIP cohort could be successfully genotyped. Individuals with low genotyping rate (<98%) and SNPs showing significant deviation from the Hardy-Weinberg equilibrium (HWE, *P* value < 1×10^{-5}) were excluded. Similarly, a low minor allele frequency (MAF;<10%) and SNPs with high rates of missing data (>2%) were excluded. This resulted in 436,643 SNPs and 160 individuals for further analysis. In the 160 samples that passed the quality control, imputation of additional variants was performed using IMPUTE v2 (Howie et al., 2009) on the basis of HapMap CEU Phase 3 (International HapMap Consortium, 2003) and 1,000 Genomes Project version June 2010 (hg18) CEU

data for ~8 million SNPs (Durbin et al., 2010). Imputed SNPs were excluded if their posterior probability averages were less than 90% for the most likely imputed genotype (INFO ≥ 0.9). SNPs were also excluded if their call rate was less than 98%, HWE *P* value was less than 1×10^{-5} and MAF < 10%. This yielded a total of 2,011,895 SNPs. To annotate SNPs for the closest gene, we used Annovar version November 2011 (Wang et al., 2010) with the RefSeq gene annotation SNP coordinates are given according to hg18.

Human DNA of the MARS cohort samples was extracted from EDTA blood samples using the Gentra Puregene Blood Kit (Qiagen) with standardized protocols. Whole-genome SNP genotyping was performed on Illumina Sentix Human-1, HumanHap300, Human610-Quad and HumanOmniExpress Genotyping BeadChips according to the manufacturer's standard protocols. Individuals as well as the genotype data have been subjected to the same quality control steps as the MPIP cohort (genotyping rate < 98%, MAF < 10%, HWE *P* value < 1×10^{-5}, SNP missingness < 98%). Missing genotype data were imputed via IMPUTE v2 based on the 1,000 Genomes Project version Nov. 2010 ALL reference panel. The MDD-related GR eSNP profile was derived from loci associated with both dexamethasone-induced differences in gene expression and MDD. It included alleles from 20 of the 23 tag eSNPs (3 SNPs diverged from HWE in the MARS sample, Table S3. Non-risk and risk alleles (according to association with depression in the PGC dataset) were coded 0 and 1, respectively, and summed in an additive fashion to create cumulative genetic risk profile scores (GRPS; 0 ,1 ,2). The MARS GRPSs ranged from 12-30.

Human DNA from participants of the DNS cohort was isolated from saliva derived from Oragene DNA self-collection kits (DNA Genotek) customized for 23andMe. DNA extraction and genotyping were performed by the National Genetics Institute (NGI), a CLIA-certified clinical laboratory and subsidiary of Laboratory Corporation of America. The Illumina HumanOmniExpress BeadChips and a custom array containing an additional ~300,000 SNPs were used to provide genome-wide data. Due to differences in genotyping array

content the DNS GRPSs included alleles from 19 of the 23 eSNPs (Table S4) and were coded in the same way as the MARS GRPSs. All SNPs used for the GRPSs had genotyping rates < 97%, MAF < 10%, HWE *P* value < 1×10^{-5} (Table S4). DNS GRPSs ranged from 10-28 and were normally distributed (Figure 7). To account for differences in ancestral background in the full sample, we used EIGENSTRAT (v, 5.0.1) (Price et al., 2006) to generate principal components and included the first 5 components as covariates in the analysis. Five participants were outliers for these components (± 6 *SD* from the mean on one of the top ten components) and hence were excluded from analyses.

DNS neuroimaging protocol.

*BOLD fMRI paradigm***.**

A widely used and reliable challenge paradigm was employed to elicit amygdala reactivity. The paradigm consists of 4 task blocks requiring face-matching interleaved with 5 control blocks requiring shape-matching (see Figure S4D). In each face-matching trial within a block, participants view a trio of faces derived from a standard set of facial affect pictures (expressing angry, fearful, surprised, or neutral emotions), and select which of the 2 faces presented on the bottom row of the display matches the target stimulus presented on the top row. Each emotion-specific block (e.g., fearful facial expressions only) consists of 6 individual trials, balanced for gender of the face. Block order is pseudo-randomized across participants. Each of the 6 face trios is presented for 4 seconds with a variable inter-stimulus interval of 2-6 seconds; total block length is 48 seconds. In the shape-matching control blocks, participants view a trio of geometric shapes (i.e., circles, horizontal and vertical ellipses) and select which of 2 shapes displayed on the bottom matches the target shape presented on top. Each control block consists of 6 different shape trios presented for 4 seconds with a fixed inter-stimulus interval of 2 seconds, comprising a total block length of 36 seconds. The total paradigm was 390 seconds in duration. Reaction times and accuracy are recorded through an MR-compatible button box.

BOLD fMRI acquisition.

Participants were scanned using a research-dedicated GE MR750 3T scanner equipped with high-power high-duty-cycle 50-mT/m gradients at 200 T/m/s slew rate, and an eight-channel head coil for parallel imaging at high bandwidth up to 1MHz at the Duke-UNC Brain Imaging and Analysis Center. A semi-automated high-order shimming program was used to ensure global field homogeneity. A series of 34 interleaved axial functional slices aligned with the anterior commissure-posterior commissure (AC-PC) plane were acquired for full-brain coverage using an inverse-spiral pulse sequence to reduce susceptibility artifact (TR/TE/flip angle = 2000 ms / 30 ms / 60; FOV = 240 mm; 3.75 × 3.75 × 4 mm voxels (selected to provide whole brain coverage while maintaining adequate signal-to-noise and optimizing acquisition times); interslice skip = 0). Four initial RF excitations were performed (and discarded) to achieve steady-state equilibrium. To allow for spatial registration of each participant's data to a standard coordinate system, high-resolution three-dimensional structural images were acquired in 34 axial slices co-planar with the functional scans (TR/TE/flip angle = 7.7s / 3.0 ms / 12; voxel size = 0.9 × 0.9 × 4 mm; FOV = 240 mm; interslice skip = 0).

BOLD fMRI data analysis.

The general linear model of Statistical Parametric Mapping 8 (SPM8) (http://www.fil.ion.ucl.ac.uk/spm) was used for whole-brain image analysis. Individual subject data were first realigned to the first volume in the time series to correct for head motion before being spatially normalized into the standard stereotactic space of the Montreal Neurological Institute (MNI) template using a 12-parameter affine model. Next, data were smoothed to minimize noise and residual differences in individual anatomy with a 6mm FWHM Gaussian filter. Voxel-wise signal intensities were ratio normalized to the whole-brain global mean. Then the ARTifact Detection Tool (ART; https://www.nitrc.org/docman/view.php/104/390/Artifact%20Detection%20Toolbox%20Manu

al) was used to generate regressors accounting for images due to large motion (i.e., > 0.6 mm relative to the previous time frame) or spikes (i.e., global mean intensity 2.5 standard deviations from the entire time series). Participants for whom more than 5% of acquisition volumes were flagged by ART (*n* = 21) were removed from analyses. An region of interest (ROI) mask (Automated Anatomical Labeling (AAL) atlas) from WFU pickatlas (Maldjian et al., 2003) was used to ensure adequate amygdala coverage for the face-matching and number-guessing tasks, respectively. Participants who had less than 90% coverage of the amygdala (*n* = 14) were excluded from analyses.

Following preprocessing steps outlined above, linear contrasts employing canonical hemodynamic response functions were used to estimate task-specific (i.e., "Angry & Fearful Faces > Neutral Faces", "Angry & Fearful > Shapes", "Neutral > Shapes") BOLD responses for each individual. The primary contrast of "Angry & Fearful > Neutral" was used to assay centromedial reactivity to cues that are conditioned social signals to threat in the environment (i.e., angry and fearful expressions) relative to signals that do not convey threat information about the environment (i.e., neutral expressions). Post-hoc analyses using the "Angry & Fearful > Shapes" and "Neutral > Shapes" contrasts were used to discern if the association with GRPS reflected relatively decreased reactivity to angry and fearful expressions or increased reactivity to neutral expressions. Individual contrast images (i.e., weighted sum of the beta images) were used in second-level random effects models accounting for scan-to-scan and participant-to-participant variability to determine mean contrast-specific responses using one-sample t-tests. A voxel-level statistical threshold of *P* value < 0.05, family wise error corrected for multiple comparisons across the bilateral centromedial amygdala ROIs, and a cluster-level extent threshold of 10 contiguous voxels was applied to these analyses. The bilateral centromedial amygdala ROIs were defined using anatomical probability maps (Amunts et al., 2005). The centromedial ROI was chosen because it includes the central nucleus of the amygdala (CeA). This specifically functions to drive physiologic, attentive, and

neuromodulatory responses to threat, as opposed to the basolateral complex of the amygdala (BLA), which primarily functions to relay information to the CeA. Thus, the expression of stress responsive behavior is more closely linked with the activity of the CeA and not the BLA (Davis and Whalen, 2001; LeDoux, 2007). Human research using such distinctions has shown that ROIs encompassing the CeA or BLA differentially respond to stimuli and share different patterns of functional as well as structural connectivity (Brown et al., 2014; Etkin et al., 2004; Lerner et al., 2012).

BOLD parameter estimates from a cluster within the left centromedial amygdala ROI exhibiting a main effect for the "Angry & Fearful > Neutral" contrast were extracted using the VOI tool in SPM8 and exported for regression analyses in SPSS (v.18). No significant cluster emerged in the right centromedial amygdala. Extracting parameter estimates from clusters activated by our fMRI paradigm, rather than those specifically correlated with our independent variables of interest, precludes the possibility of any correlation coefficient inflation that may result when an explanatory covariate is used to select a region of interest. We have successfully used this strategy in prior studies (Bogdan et al., 2012).

Statistical Analysis.

Cis-associations of baseline gene expression.

Using baseline gene expression of the 4,447 differently regulated autosomal array probes (absolute fold change ≥ 1.3 in at least 20% of all samples), 26,205 unique *cis*-SNPs and 764 gene expression probes corresponding to 31,541 *cis*-eQTLs were found to be significant after multiple testing correction with the same strategy as described for the GR-stimulated gene expression changes. The 26,205 unique eSNPs represented 1,010 uncorrelated eSNP bins (1,148 eSNP bin-probe combinations). The 775 eQTL bins (68%) were located within 100 kb upstream or downstream from the array probe ends, 911 eQTL bins (79%) within 200 kb and only 237 eQTLs bins > 200 kb (21%).

Validation GR-response cis-eQTL results

Validation of GR-response *cis*-eQTL results was carried out with a sample size-weighted Z-score meta-analysis (Evangelou and Ioannidis, 2013) in an additional independent data set using peripheral blood samples (baseline and after GR-stimulation with 1.5 mg dexamethasone) of 58 individuals (21 male controls, 14 male cases and 23 female cases). We applied the same strategy as used in the discovery sample (MPIP cohort) to filter, normalize and batch correct the gene expression data. We adjusted the analysis for the same covariates plus gender; applied the same SNP quality control checks and performed the *cis*-eQTL mapping in PLINK.

Enrichment of GR binding regions

To identify whether GR-response eSNPs were enriched for GR binding sites, we used the *E*NCODE (ENCODE Project Consortium, 2011) *NR3C1* ChIP-seq data from GM12878 LCLs (accession: ENCSR904YPP) from which no aligned tracks are currently available. Raw data were download at https://www.encodeproject.org/experiments and initial filtering was performed using FASTX Toolkit (v. 0.0.14, http://hannonlab.cshl.edu/fastx_toolkit/index.html) and Prinseq (v. 0.20.3) (Schmieder and Edwards, 2011) to eliminate artifacts and low quality reads. Alignment on hg19 was performed using BWA (v. 0.7.10) (Li and Durbin, 2009) allowing only uniquely mappable alignments with alignment quality of above 20. Reads from both ChIP and both control libraries were pooled leading to 46,453,650 and 68,227,580 used reads, respectively. Peak-calling was carried out by MACS14 (v. 1.4.2) (Zhang et al., 2008) using default settings, resulting in around 23,000 annotated signals. The average length of a ChIP signal as defined by the peak calling was 746.3 bps ± 370.6 bsp.

We mapped the GR-response eSNPs to these GR ChIP-seq peaks and compared the overlap observed with 1,000 equal sized sets of randomly drawn SNPs (n=3,662 SNPs) from of all analyzed SNPs (without replacement) matched in MAF (=null distribution). To match the MAF distributions of the random SNP sets with our GR-response eQTL data we

divided the SNPs into non-overlapping MAF bins, each of the width 0.05 as described previously (Nicolae et al., 2010). For every set we counted the percentage of SNPs within a GR ChIP-seq peak. Enrichment calculations with a permutation-based *FDR* < 10% were considered as statistically significant within the entire manuscript.

Enhancer enrichment analysis

We investigated whether GR-response eSNP binds are enriched for functional enhancer annotations using the online tool HaploReg version 2 (Ward and Kellis, 2012) based on the Roadmap Epigenome data (Roadmap Epigenomics Consortium et al., 2015) and using the 1,000 Genomes Project CEU data as a background data set. Additionally we performed the enrichment analysis on ten permuted baseline eSNP bin sets (size matched) to generate a realistic null distribution. The average enhancer enrichment over the ten permutations is present in Figure 3 and S2.

Chromatin interaction analysis with paired-end tag (ChIA-PET) mapping.

The combined set of the first two replicates of the RNA Polymerase II ChIA-PET data (Li et al., 2010; 2012) generated from K562 chronic myeloid leukemia cell lines (*n* > 400,000 interaction regions) was obtained from the UCSC Genome Browser (http://hgdownload.cse.ucsc.edu/goldenPath/hg19/encodeDCC/wgEncodeGisChiaPet/). Genomic coordinates of our GR-response eSNP bins were converted from hg18 to GRCh build 37 (hg19) using the UCSC Genome Browser liftOver tool (http://genome.ucsc.edu/cgi-bin/hgLiftOver) and the probe gene coordinates were updated with the hg19 RefSeq (Pruitt et al., 2012) gene table obtained from the UCSC Table Browser (http://hgdownload.soe.ucsc.edu/goldenPath/hg19/database/refGene.txt.gz; excluding 15 probe genes on hg19). To estimate the overlap of the direct chromatin interactions and GR-response eQTL bins (eSNP bin-probe gene combination) we tested if one ChIA-PET tag overlapped with the region of the eSNP bin ± 10kb as well as the relevant array probe gene

(10kb ± transcription start or end). To establish the null distribution, we permuted the distances between the GR-response eSNP bins and the transcription sites of the corresponding probe gene (*n* = 270 updated to hg19) and estimated the overlap with ChIA-PET interaction signals. We repeated the analysis 1,000 times and for each set we counted the number of genes with overlapping ChIA-PET data.

Enrichment of GWAS susceptibility markers.

To identify whether GR-response eSNPs were specifically enriched for association with psychiatric disorders and not with other diseases or traits, we generated 1,000 sets of permuted baseline eSNPs (conditional on MAF and number of GR-response eSNPs overlapping with the respective GWAS). For every set we counted the percentage of unique SNPs with a GWAS results at *P* value ≤ 0.05. On this basis we constructed the null distribution. A second null distribution was created based on all imputed SNPs of high quality.

1.) PGC MDD data: The MDD GWAS data was generated by conducting a meta-analysis based on the Psychiatric Genomics Consortium (PGC) GWAS mega-analysis for MDD (Major Depressive Disorder Working Group of the Psychiatric GWAS Consortium, 2012) data . We used the “meta-analysis” function in PLINK assuming a fixed effect model in 17,846 individuals of European ancestry (8,864 cases with MDD and 8,982 controls) from 8 of the 9 studies included in the PGC MDD data. All samples from the initial PGC MDD data (*n* = 18,759) that overlapped with our MARS cohort (*n* = 376 cases and 537 controls) were excluded, which was then used as validation sample. The PGC MDD analysis used SNP data imputed to the 1,000 Genomes Project (hg19).

2.) PGC cross-disorder data: The results of the PGC cross-disorder (CD) analysis (33,332 patients and 27,888 controls of European ancestry distributed among five disorders: SCZ, BPD, ADHD, ASD and MDD) (Cross-Disorder Group of the Psychiatric Genomics

Consortium, 2013; Cross-Disorder Group of the Psychiatric Genomics Consortium et al., 2013) were obtained from the PGC website (http://pgc.unc.edu). The PGC CD analysis applied a multinomial regression procedure and used SNP data imputed to the HapMap Phase 3 data (hg18).

3.) PGC SCZ2 data: The results of the multistage GWAS for SCZ (Schizophrenia Working Group of the Psychiatric Genomics, 2014) obtained from the PGC website (http://pgc.unc.edu). The PGC SCZ2 analysis used SNP data imputed to the 1,000 Genomes Project (hg19).

4.) Non psychiatric trait data: The GWAS data for height (Heid et al., 2010) and rheumatoid arthritis (RA) (Stahl et al., 2010) were obtained from the PGC website (http://pgc.unc.edu). Results of the Crohn's disease (CD) analysis were obtained from International Inflammatory Bowel Disease Genetics Consortium website (http://www.ibdgenetics.org). The RA analysis used SNP data imputed to the HapMap Phase 2 data (hg17) and the CD as well as height data was imputed based on HapMap Phase 3. For comparability we converted all our SNP coordinates to the relevant genome assembly of analyzed GWAS data using the UCSC Genome Browser liftOver tool.

Co-expression analysis

For the co-expression analysis we used the GR-response residuals from all array probes (*n* = 4,447) to determine if the 25 MDD-related GR array probes are more co-regulated than 1,000 sets of randomly chosen GR-stimulated transcripts. To realize this, we carried out a co-expression analysis in R using the function "dist" specifying the Euclidian distance as distance measure and calculated the mean distance of all pair-wise distances. We established the significance of co-expression network of the 25 MDD-related GR array probes by testing the observed mean distance versus the null distributions created by

calculating the mean distance of all pair-wise distances for 1,000 sets of 25 randomly chosen GR-stimulated transcripts. Next, we determined the number of sets, having lower mean distances than the actual MDD-related GR transcripts to measure the enrichment statistic.

*DNS neuroimaging analysis***.**

Statistical analyses of the imaging data were completed using linear regression in SPSS to test the association of the MDD-related GR tag eSNP GRPSs to amygdala reactivity in the independent DNS cohort. To maintain variability but constrain the influence of extreme outliers, prior to any analyses, all imaging variables were winsorized (i.e., following data quality control procedures, outliers more than ± 3 SD were set at ± 3 SD from the mean; for the "Angry and Fearful > Neutral faces" contrast, 13 outliers (2.01%) of the entire sample were moved to ± 3 SD from the mean). Gender, psychiatric diagnosis (0,1) and age were entered as covariates for both EUR-AM and entire sample analyses. Five ancestrally-informative principal components that distinguish the sample were added as additional covariates in the analyses of the entire sample. We computed permutations (n = 1,000) in which we constructed randomly generated SNP profiles that were matched for MAF, amount of SNPs (n = 19) and constrained by the max LD observed within the sample.

Graphs were generated with Haploview (Barrett et al., 2005), ggplot2 ((Wickham, 2009) and Circos (Krzywinski et al., 2009).

Chromatin conformation capture

Five human lymphoblastoid cell lines were cultured in RMPI media with stable l-glutamine (Biochrom) supplemented with 10% fetal bovine serum and 1% antibiotic-antimycotic (Life Technologies). Crosslinking and cell lysis were performed as described (Hagège et al., 2007). Nuclei were digested using 1,000 U of *Nco*I. Subsequent re-ligation, de-crosslinking and purification were conducted according to the manufacturer's protocol. Following assessment of digestion efficiency and sample purity, DNA concentration of the 3C samples

were determined by SybrGreen quantitative PCR using an “internal” primer set (see Table S6; primers that do not amplify across sites recognized by the restriction enzyme used) as described in (Hagège et al., 2007). Primers were designed with an anchor primer in the fragment containing the TSS of *LONP1* and in potential interacting fragments in and around eSNP bin of *NRTN* using Primer3Plus (http://www.bioinformatics.nl/cgi-bin/primer3plus/primer3plus.cgi). Quantitative PCR was carried out using ABsolute Blue qPCR SYBR Green Master Mix (Thermo Fisher Scientific) and the Mini Opticon Real-Time PCR System (Bio-Rad) according to the manufacturer’s instructions. A 179-kb BAC clone (CTD-2522A4) containing the entire *LONP1-NRTN* genomic sequence was purchased from Life Technologies and served as PCR control template. The BAC clone was cut with *Nco*I and re-ligated by T4 DNA ligase. All primer pairs were tested on a standard curve of the BAC control library and yielded PCR efficiencies > 1.7. The presence of a single PCR product was confirmed by agarose gel electrophoresis and melting curve analysis. Cycling conditions were: 95 °C for 15min, 45 cycles of 95°C for 15s, 60°C for 15s, 72°C for 15s. Quantitative PCR data were normalized to *GAPDH* as a loading control. *GAPDH* cycling conditions were 95 °C for 15min, 45 cycles of 95°C for 15s, 60°C for 15s, 72°C for 15s. Data analysis was carried out according to (Hagège et al., 2007) and is presented as relative crosslinking frequency. Primers used for the chromatin conformation capture interaction studies are listed in Table S6. Linear mixed models were used for statistical analysis.

Quantitative real-time PCR (qPCR) validation.

Total RNA was reverse-transcribed to cDNA using random primers and the Superscript II reverse transcriptase (Invitrogen) for qPCR to validate microarray results. qPCR was carried out according to manufactures instructions using Roche-LightCycler 480 System (Roche Applied Science) and assays were designed using the Roche Universal Probe Library (http://qpcr.probefinder.com) for *ADORA3* (the probe with a significant GR-response eQTLs), *HIST2H2AA3/4* (the probe with the most eSNPs overlapping with the meta-analysis results

for MDD) and *TBP* as the endogenous control gene. Assays for *LONP1* and *GADPH* were designed using Primer3Plus (http://www.bioinformatics.nl/cgi-bin/primer3plus/primer3plus.cgi). The association between eSNPs and GR-stimulated gene expression of the target genes could be validated using qPCR (see Figure 2C,D and 4A,B). Sequences of primers used are summarized in Table S6. All samples were run in duplicates and duplicates discordant in *CT* values by more than 0.2 cycles, were excluded from the analysis. Relative gene transcript levels were determined by Pfaffl's equation (Pfaffl, 2001) with: $\text{ratio} = \frac{(\text{E}_{\text{gene}})^{\Delta\text{CT}_{\text{gene}}(\text{baseline sample} - GR-\text{stimulated sample})}}{(\text{E}_{\text{housekeeper}})^{\Delta\text{CT}_{\text{housekeeper}}(\text{baseline sample} - GR-\text{stimulated sample})}}$. qPCR ratios shown in Figure 2D and were calculated using the following equations:

$$pre = \frac{(E_{housekeeper})^{CT_{housekeeper}(baseline\ sample)}}{(E_{gene})^{CT_{gene}(baseline\ sample)}}$$

and *post* = $\frac{(E_{housekeeper})^{CT_{housekeeper}(GR-stimulated\ sample)}}{(E_{gene})^{CT_{gene}(GR-stimulated\ sample)}}$.

qPCR validation results.

Two transcript variants encoding isoforms with a different 3'UTR length have been identified for *HIST2H2AA3/4*. The shorter gene product (isoform 1) is annotated by RefSeq while the alternatively spliced longer gene product (isoform 2) is annotated by Ensembl release 54 (HIST2H2AA3-001; ENST00000369161) and further predicted by AceView (HIST2H2AA3.aApr07-unspliced, HIST2H2AA4.aApr07-unspliced). This longer isoform is tagged by the significant Illumina probe (ILMN_1695435). Hence we designed two different assays- one covering the common part of both isoforms (assay 1) and the other tagging isoform 2 (assay 2). The expression levels measured with both assays were highly correlated (Spearman's test *P* value < 1.5×10^{-20}, *R* = 74%). We could replicate a significant SNP effect in 137 samples with a *P* value of 0.012 using assay 1 with a genotypic model and *P* = 0.017 using a carrier model, with the same direction of change as in the expression array.

SUPPLEMENTAL REFERENCES

Amunts, K., Kedo, O., Kindler, M., Pieperhoff, P., Mohlberg, H., Shah, N.J., Habel, U., Schneider, F., and Zilles, K. (2005). Cytoarchitectonic mapping of the human amygdala, hippocampal region and entorhinal cortex: intersubject variability and probability maps. Anat. Embryol. *210*, 343–352.

Barbosa-Morais, N.L., Dunning, M.J., Samarajiwa, A.S., Darot, J.F.J., Ritchie, M.E., Lynch, A.G., and Tavaré, S. (2010). A re-annotation pipeline for Illumina BeadArrays: improving the interpretation of gene expression data. Nucleic Acids Res. *38*, e17.

Barrett, J.C., Fry, B., Maller, J., and Daly, M.J. (2005). Haploview: analysis and visualization of LD and haplotype maps. Bioinformatics *21*, 263–265.

Bogdan, R., Williamson, D.E., and Hariri, A.R. (2012). Mineralocorticoid receptor Iso/Val (rs5522) genotype moderates the association between previous childhood emotional neglect and amygdala reactivity. Am J Psychiat *169*, 515–522.

Brown, V.M., Labar, K.S., Haswell, C.C., Gold, A.L., McCarthy, G., Morey, R.A., and Workgrp, M.-A.M. (2014). Altered Resting-State Functional Connectivity of Basolateral and Centromedial Amygdala Complexes in Posttraumatic Stress Disorder. Neuropsychopharmacology *39*, 351–359.

Cross-Disorder Group of the Psychiatric Genomics Consortium (2013). Identification of risk loci with shared effects on five major psychiatric disorders: a genome-wide analysis. The Lancet *381*, 1371–1379.

Cross-Disorder Group of the Psychiatric Genomics Consortium, Lee, S.H., Ripke, S., Neale, B.M., Faraone, S.V., Purcell, S.M., Perlis, R.H., Mowry, B.J., Thapar, A., Goddard, M.E., et al. (2013). Genetic relationship between five psychiatric disorders estimated from genome-wide SNPs. Nat Genet *45*, 984–994.

Davis, M., and Whalen, P.J. (2001). The amygdala: vigilance and emotion. Molecular Psychiatry *6*, 13–34.

Durbin, R.M., Altshuler, D.L., Durbin, R.M., Abecasis, G.R., Bentley, D.R., Chakravarti, A., Clark, A.G., Collins, F.S., La Vega, De, F.M., Donnelly, P., et al. (2010). A map of human genome variation from population-scale sequencing. Nature *467*, 1061–1073.

ENCODE Project Consortium (2011). A user's guide to the encyclopedia of DNA elements (ENCODE). PLoS Biol. *9*, e1001046.

Etkin, A., Klemenhagen, K.C., Dudman, J.T., Rogan, M.T., Hen, R., Kandel, E.R., and Hirsch, J. (2004). Individual differences in trait anxiety predict the response of the basolateral amygdala to unconsciously processed fearful faces. Neuron *44*, 1043–1055.

Evangelou, E., and Ioannidis, J.P.A. (2013). Meta-analysis methods for genome-wide association studies and beyond. Nature Reviews Genetics *14*, 379–389.

First, M.B., Gibbon, M., Spitzer, R.L., Williams, J.W.B., and Benjamin, L.S. (1997). Structured Clinical Interview for DSM-IV Axis II Personality Disorders, (SCID-II). Washington, D.C.: American Psychiatric Press, Inc.

Hagège, H., Klous, P., Braem, C., Splinter, E., Dekker, J., Cathala, G., de Laat, W., and Forné, T. (2007). Quantitative analysis of chromosome conformation capture assays (3C-qPCR). Nat Protoc *2*, 1722–1733.

Heid, I.M., Jackson, A.U., Randall, J.C., Winkler, T.W., Qi, L., Steinthorsdottir, V., Thorleifsson, G., Zillikens, M.C., Speliotes, E.K., Mägi, R., et al. (2010). Meta-analysis identifies 13 new loci associated with waist-hip ratio and reveals sexual dimorphism in the genetic basis of fat distribution. Nat Genet *42*, 949–960.

Hennings, J.M., Owashi, T., Binder, E.B., Horstmann, S., Menke, A., Kloiber, S., Dose, T., Wollweber, B., Spieler, D., Messer, T., et al. (2009). Clinical characteristics and treatment outcome in a representative sample of depressed inpatients-findings from the Munich Antidepressant Response Signature (MARS) project. J Psychiatr Res *43*, 215–229.

Howie, B.N., Donnelly, P., and Marchini, J. (2009). A flexible and accurate genotype imputation method for the next generation of genome-wide association studies. PLoS Genet *5*, e1000529.

International HapMap Consortium (2003). The International HapMap Project. Nature *426*, 789–796.

Ising, M., Lucae, S., Binder, E.B., Bettecken, T., Uhr, M., Ripke, S., Kohli, M.A., Hennings, J.M., Horstmann, S., Kloiber, S., et al. (2009). A genomewide association study points to multiple loci that predict antidepressant drug treatment outcome in depression. Archives of General Psychiatry *66*, 966–975.

Johnson, W.E., and Cheng, L. (2007). Adjusting batch effects in microarray expression datausing empirical Bayes methods. Biostatistics *8*, 118–127.

Krawiec, J.A., Chen, H., Alom-Ruiz, S., and Jaye, M. (2009). Modified PAXgene (TM) method allows for isolation of high-integrity total RNA from microlitre volumes of mouse whole blood. Lab. Anim. *43*, 394–398.

Krzywinski, M., Schein, J., Birol, I., Connors, J., Gascoyne, R., Horsman, D., Jones, S.J., and Marra, M.A. (2009). Circos: an information aesthetic for comparative genomics. Genome Research *19*, 1639–1645.

LeDoux, J. (2007). The amygdala. Curr. Biol. *17*, R868–R874.

Leek, J.T., and Storey, J.D. (2007). Capturing heterogeneity in gene expression studies by surrogate variable analysis. PLoS Genet *3*, 1724–1735.

Lerner, Y., Singer, N., Gonen, T., Weintraub, Y., Cohen, O., Rubin, N., Ungerleider, L.G., and Hendler, T. (2012). Feeling without Seeing? Engagement of Ventral, but Not Dorsal, Amygdala during Unaware Exposure to Emotional Faces. Journal of Cognitive Neuroscience *24*, 531–542.

Li, G., Fullwood, M.J., Xu, H., Mulawadi, F.H., Velkov, S., Vega, V., Ariyaratne, P.N., Mohamed, Y.B., Ooi, H.-S., Tennakoon, C., et al. (2010). ChIA-PET tool for comprehensive chromatin interaction analysis with paired-end tag sequencing. Genome Biol *11*, R22.

Li, G., Ruan, X., Auerbach, R.K., Sandhu, K.S., Zheng, M., Wang, P., Poh, H.M., Goh, Y., Lim, J., Zhang, J., et al. (2012). Extensive promoter-centered chromatin interactions provide

a topological basis for transcription regulation. Cell *148*, 84–98.

Li, H., and Durbin, R. (2009). Fast and accurate short read alignment with Burrows-Wheeler transform. Bioinformatics *25*, 1754–1760.

Lin, S.M., Du, P., Huber, W., and Kibbe, W.A. (2008). Model-based variance-stabilizing transformation for Illumina microarray data. Nucleic Acids Res. *36*, e11.

Major Depressive Disorder Working Group of the Psychiatric GWAS Consortium (2012). A mega-analysis of genome-wide association studies for major depressive disorder. Molecular Psychiatry *18*, 497–511.

Maldjian, J.A., Laurienti, P.J., Kraft, R.A., and Burdette, J.H. (2003). An automated method for neuroanatomic and cytoarchitectonic atlas-based interrogation of fMRI data sets. Neuroimage *19*, 1233–1239.

Menke, A., Arloth, J., Pütz, B., Weber, P., Klengel, T., Mehta, D., Gonik, M., Rex-Haffner, M., Rubel, J., Uhr, M., et al. (2012). Dexamethasone Stimulated Gene Expression in Peripheral Blood is a Sensitive Marker for Glucocorticoid Receptor Resistance in Depressed Patients. Neuropsychopharmacology *37*, 1455–1464.

Nicolae, D.L., Gamazon, E., Zhang, W., Duan, S., Dolan, M.E., and Cox, N.J. (2010). Trait-associated SNPs are more likely to be eQTLs: annotation to enhance discovery from GWAS. PLoS Genet *6*, e1000888.

Paxinos, G., and Franklin, K.B.J. (2003). The mouse brain in stereotaxic coordinates. Academic Press; 2 Edition.

Pfaffl, M.W. (2001). A new mathematical model for relative quantification in real-time RT-PCR. Nucleic Acids Res. *29*, e45.

Price, A.L., Patterson, N.J., Plenge, R.M., Weinblatt, M.E., Shadick, N.A., and Reich, D. (2006). Principal components analysis corrects for stratification in genome-wide association studies. Nat Genet *38*, 904–909.

Pruitt, K.D., Tatusova, T., Brown, G.R., and Maglott, D.R. (2012). NCBI Reference Sequences (RefSeq): current status, new features and genome annotation policy. Nucleic Acids Res. *40*, D130–D135.

Roadmap Epigenomics Consortium, Kundaje, A., Meuleman, W., Ernst, J., Bilenky, M., Yen, A., Heravi-Moussavi, A., Kheradpour, P., Zhang, Z., Wang, J., et al. (2015). Integrative analysis of 111 reference human epigenomes. Nature *518*, 317–330.

Schizophrenia Working Group of the Psychiatric Genomics (2014). Biological insights from 108 schizophrenia-associated genetic loci. Nature *511*, 421–427.

Schmieder, R., and Edwards, R. (2011). Quality control and preprocessing of metagenomic datasets. Bioinformatics *27*, 863–864.

Sheehan, D.V., Lecrubier, Y., Sheehan, K.H., Amorim, P., Janavs, J., Weiller, E., Hergueta, T., Baker, R., and Dunbar, G.C. (1998). The Mini-International Neuropsychiatric Interview (M.I.N.I.): the development and validation of a structured diagnostic psychiatric interview for DSM-IV and ICD-10. J Clin Psychiatry *59 Suppl 20*, 22–33–quiz34–57.

Spijker, S. (2011). Dissection of Rodent Brain Regions. In Neuroproteomics, (Totowa, NJ: Humana Press), pp. 13–26.

Stahl, E.A., Raychaudhuri, S., Remmers, E.F., Xie, G., Eyre, S., Thomson, B.P., Li, Y., Kurreeman, F.A.S., Zhernakova, A., Hinks, A., et al. (2010). Genome-wide association study meta-analysis identifies seven new rheumatoid arthritis risk loci. Nat Genet *42*, 508–514.

Wagner, K.V., Hartmann, J., Mangold, K., Wang, X.-D., Labermaier, C., Liebl, C., Wolf, M., Gassen, N.C., Holsboer, F., Rein, T., et al. (2013). Homer1 mediates acute stress-induced cognitive deficits in the dorsal hippocampus. J. Neurosci. *33*, 3857–3864.

Wang, K., Li, M., and Hakonarson, H. (2010). ANNOVAR: functional annotation of genetic variants from high-throughput sequencing data. Nucleic Acids Res. *38*, e164.

Ward, L.D., and Kellis, M. (2012). HaploReg: a resource for exploring chromatin states, conservation, and regulatory motif alterations within sets of genetically linked variants. Nucleic Acids Res. *40*, D930–D934.

Wickham, H. (2009). ggplot2: Elegant Graphics for Data Analysis (Springer Publishing Company, Incorporated).

Zhang, Y., Liu, T., Meyer, C.A., Eeckhoute, J., Johnson, D.S., Bernstein, B.E., Nusbaum, C., Myers, R.M., Brown, M., Li, W., et al. (2008). Model-based analysis of ChIP-Seq (MACS). Genome Biol *9*, R137.

SUPPLEMENTAL NOTES

List of collaborators of the Major Depressive Disorder Working Group of the Psychiatric Genomics Consortium.

#	First name	Last name	Affiliation	#	First name	Last name	Affiliation
1	Stephan	Ripke	Harvard University/Broad Institute	59	Michel	Guipponi	University of Geneva
2	Naomi R	Wray	Queensland Institute of Medical Research/University of Queen	60	Anjali K	Henders	Queensland Institute of Medical Research
3	Cathryn M	Lewis	Institute of Psychiatry, King's College London	61	Stefan	Herms	University of Bonn
4	Steven P	Hamilton	University of California, San Francisco	62	Ian B	Hickie	University of Sydney, Sydney
5	Myrna M	Weissman	Columbia University	63	Susanne	Hoefels	University of Bonn
6	Gerome	Breen	Institute of Psychiatry, King's College London	64	Witte	Hoogendijk	Erasmus Medical Center
7	Enda M	Byrne	Queensland Institute of Medical Research	65	Jouke Jan	Hottenga	VU University, Amsterdam
8	Douglas HR	Blackwood	University of Edinburgh	66	Dan V	Iosifescu	Massachusetts General Hospital
9	Dorret I	Boomsma	VU University, Amsterdam	67	Marcus	Ising	Max Planck Institute of Psychiatry
10	Sven	Cichon	University of Bonn	68	Ian	Jones	Cardiff University
11	Andrew C	Heath	Washington University, St Louis	69	Lisa	Jones	University of Birmingham
12	Florian	Holsboer	Max Planck Institute of Psychiatry	70	Tzeng	Jung-Ying	North Carolina State University
13	Susanne	Lucae	Max Planck Institute of Psychiatry	71	James A	Knowles	University of Southern California
14	Pamela AF	Madden	Washington University, St Louis	72	Isaac S	Kohane	Brigham and Women's Hospital
15	Nicholas G	Martin	Queensland Institute of Medical Research	73	Martin A	Kohli	Max Planck Institute of Psychiatry
16	Peter	McGuffin	Institute of Psychiatry, King's College London	74	Ania	Korszun	Queen Mary University of London
17	Pierandrea	Muglia	GlaxoSmithKline	75	Mikael	Landen	Karolinska Institutet
18	Markus M	Noethen	University of Bonn	76	William B	Lawson	Howard University
19	Brenda P	Penninx	VU University Medical Center, Amsterdam	77	Glyn	Lewis	University of Bristol
20	Michele L	Pergadia	Washington University, St Louis	78	Donald	MacIntyre	University of Edinburgh
21	James B	Potash	University of Iowa	79	Wolfgang	Maier	University of Bonn
22	Marcella	Rietschel	Central Inst Mental Health, University of Heidelberg	80	Manuel	Mattheisen	University of Bonn
23	Danyu	Lin	University of North Carolina	81	Patrick J	McGrath	Columbia University
24	Bertram	Müller-Myhsok	Max Planck Institute of Psychiatry	82	Andrew	McIntosh	University of Edinburgh
25	Jianxin	Shi	National Cancer Institute	83	Alan	McLean	University of Edinburgh
26	Stacy	Steinberg	deCODE Genetics	84	Christel M	Middeldorp	VU University, Amsterdam
27	Hans J	Grabe	University of Greifswald	85	Lefkos	Middleton	Imperial College
28	Paul	Lichtenstein	Karolinska Institutet	86	Grant M	Montgomery	Queensland Institute of Medical Research
29	Patrik	Magnusson	Karolinska Institutet	87	Shawn N	Murphy	Massachusetts General Hospital
30	Roy H	Perlis	Massachusetts General Hospital	88	Matthias	Nauck	University of Greifswald
31	Martin	Preisig	University of Lausanne	89	Willem A	Nolen	Groningen University Medical Center
32	Jordan W	Smoller	Massachusetts General Hospital	90	Dale R	Nyholt	Queensland Institute of Medical Research
33	Kari	Stefansson	deCODE Genetics	91	Michael	O'Donovan	Cardiff University
34	Rudolf	Uher	Institute of Psychiatry, King's College London	92	Högni	Oskarsson	Therapeia, University Hospital
35	Zoltan	Kutalik	University of Lausanne	93	Nancy	Pedersen	Karolinska Institutet
36	Katherine E	Tansey	Institute of Psychiatry, King's College London	94	William A	Scheftner	Rush University Medical Center
37	Alexander	Teumer	University of Greifswald	95	Andrea	Schulz	University of Greifswald
38	Alexander	Viktorin	Karolinska Institutet	96	Thomas G	Schulze	University of Goettingen
39	Michael R	Barnes	GlaxoSmithKline	97	Stanley I	Shyn	University of Washington
40	Thomas	Bettecken	Max Planck Institute of Psychiatry	98	Engilbert	Sigurdsson	Landspitali University Hospital
41	Elisabeth B	Binder	Max Planck Institute of Psychiatry	99	Susan L	Slager	Mayo Clinic
42	René	Breuer	Central Inst Mental Health, University of Heidelberg	100	Johannes H	Smit	VU University Medical Center, Amsterdam
43	Victor M	Castro	Partners HealthCare System	101	Hreinn	Stefansson	deCODE Genetics
44	Susanne E	Churchill	Partners HealthCare System	102	Michael	Steffens	University of Bonn
45	William H	Coryell	University of Iowa	103	Thorgeir	Thorgeirsson	deCODE Genetics
46	Nick	Craddock	Cardiff University	104	Federica	Tozzi	GlaxoSmithKline
47	Ian W	Craig	Institute of Psychiatry, King's College London	105	Jens	Treutlein	Central Inst Mental Health, University of Heidelberg
48	Darina	Czamara	Max Planck Institute of Psychiatry	106	Manfred	Uhr	Max Planck Institute of Psychiatry
49	Eco J	De Geus	VU University, Amsterdam	107	Edwin JCG	van den Oord	Virginia Commonwealth University
50	Franziska	Degenhardt	University of Bonn	108	Gerard	Van Grootheest	VU University Medical Center, Amsterdam
51	Anne E	Farmer	Institute of Psychiatry, King's College London	109	Henry	Völzke	University of Greifswald
52	Maurizio	Fava	Massachusetts General Hospital	110	Jeffrey B	Weilburg	Massachusetts General Hospital
53	Josef	Frank	Central Inst Mental Health, University of Heidelberg	111	Gonneke	Willemsen	VU University, Amsterdam
54	Vivian S	Gainer	Partners HealthCare System	112	Frans G	Zitman	Leiden University Medical Center, Leiden
55	Patience J	Gallagher	Massachusetts General Hospital	113	Benjamin	Neale	Harvard University/Broad Institute
56	Scott D	Gordon	Queensland Institute of Medical Research	114	Mark	Daly	Harvard University/Broad Institute
57	Sergey	Goryachev	Partners HealthCare System	115	Douglas F	Levinson	Stanford University
58	Magdalena	Gross	University of Bonn	116	Patrick F	Sullivan	University of North Carolina